**Table VII.** Electrochemical Data for $Ni^{3+/2+}$ Couples in an 0.5 M Sulfate Medium, vs SCE

| complex | $E_{1/2}$, V | ref | complex | $E_{1/2}$, V | ref |
|---|---|---|---|---|---|
| [Ni(L1)] | 0.76 | this work | [Ni(L5)] | 0.10 | 6 |
| [Ni(cyclam)] | 0.50 | 11 | [Ni(L6)] | 0.61 | 31 |
| [Ni(L4)] | 0.35 | 32 | [Ni(L7)] | 0.54 | 7 |

$Li_2SO_4$), and two reversible waves in $CH_3CN$ (0.1 M ($n$-$Bu)_4NPF_6$), corresponding to the $Ni^{2+/+}$ couple (-1.675 V vs $Fc^{+/0}$) and the $Ni^{3+/2+}$ couple (0.775 V vs $Fc^{+/0}$) (see Figure 6). The difference between these waves (2.45 V) is in good agreement with that observed by other workers for a variety of nickel macrocyclic complexes.[48,49]

Direct comparisons can be made between [16]-aneSN$_4$ and L1 to determine the effect of the additional chelate ring on the stability of the complex. The $E_{1/2}$ of the $[Ni([16]\text{-aneSN}_4)]^{3+/2+}$ couple has been reported as 0.77 V vs SCE in 0.5 M $Na_2SO_4$,[11] which is identical with the value obtained in this work; thus, no effect is apparent. However, it is well documented that replacement of a secondary with a tertiary amine donor in a tetraaza ring destabilizes the Ni(III) state by approximately 100 mV.[49] Therefore the additional six-membered chelate ring imparts an extra stabilization of ≈200 mV on the Ni(III) complex over that expected for a di-*N*-alkyl derivative of [16]-aneSN$_4$. The extra stability for the Ni(III) state can be attributed to two factors.

(1) The additional chelate ring, creating a macrobicycle, leads to the cryptate effect.

(2) The formation of the 14-membered $N_4$ ring results in stronger in-plane interactions, thereby raising the energy of the $e_g$ orbitals and making it easier to remove an electron from the metal center.

Both of these effects result in a greater ligand field being exerted on the metal center as observed in the UV-vis spectrum of the M(II)L1 complexes.

It is also of interest to compare the $E_{1/2}$ value for the $[Ni(L1)(X)]^{3+/2+}$ couple with that of other $Ni^{II}$(cyclam) derivatives with a single pendant arm. These are presented in Table VII. The series can be divided into two classes, those with negatively charged pendant arm donors (Ni(L4) and Ni(L5)) that have $E_{1/2}$ values lower than that of $Ni(cyclam)^{2+}$ due to their $\sigma$-donation ability and those with neutral donors that have $E_{1/2}$ values greater than that of $Ni(cyclam)^{2+}$. The order of the latter series reflects the $\pi$-donor ability of the axial ligand, stabilizing the Ni(III) center in the order imidazole > pyridine > thioether.

**Acknowledgment.** We thank, the NSERC (Canada) and the University of Victoria for support. D.G.F. was the recipient of a NSERC Post Graduate Fellowship.

**Registry No.** **1**, 118459-51-1; **2**, 118459-52-2; L1, 118459-53-3; [9]-aneSN$_2$, 88194-17-6; $BH_3$·THF, 14044-65-6; Cu(**2**)$(ClO_4)_2$, 118459-55-5; $[Cu(L1)](ClO_4)_2$, 118459-57-7; $[Ni(L1)](ClO_4)_2$, 118459-59-9; $[Ni(L1)]^{3+}$, 118459-60-2; $Co^{3+}$, 22541-63-5; $NO^+$, 14452-93-8; $[Ni^{II}(L1)H_2O]^{2+}$, 118459-63-5; $[Ni^{III}(L1)H_2O]^{3+}$, 118459-61-3; $[Ni^{III}(L1)F]^{2+}$, 118459-62-4; acrylonitrile, 107-13-1; glyoxal, 107-22-2.

**Supplementary Material Available:** Tables S1-S6, containing anisotropic temperature parameters, selected intermolecular distances, hydrogen atom fractional atomic coordinates and isotropic temperature parameters, interatomic distances and bond angles involving the hydrogen atoms, and mean planes calculations, and Table S9, containing experimental crystallographic data for both complexes (11 pages); Tables S7 and S8, listing calculated and observed structure factors (22 pages). Ordering information is given on any current masthead page.

(48) Sabatini, L.; Fabbrizzi, L. *Inorg. Chem.* **1979**, *18*, 438.
(49) Barefield, E. K.; Freeman, G. M.; Van Derveer, D. G. *Inorg. Chem.* **1986**, *25*, 552.

Contribution from the School of Chemistry,
University of Hyderabad, Hyderabad 500 134, India

# Silver(II) Complexes of Hindered N-Heterocyclic Ligands. Electron Spin Resonance of Nitrato(6,6′-dimethyl-2,2′-bipyridine)silver(II) and Nitrato(2,9-dimethyl-1,10-phenanthroline)silver(II) Ions

G. Swarnabala and M. V. Rajasekharan*

*Received April 19, 1988*

$AgLNO_3$ complexes, with L = 6,6′-dimethyl-2,2′-bipyridine (dmbp) and 2,9-dimethyl-1,10-phenanthroline (dmp), have been prepared and oxidized by peroxodisulfate to give silver(II) complex ions that have been isolated as the magnetically dilute salts $[AgLNO_3]PF_6{\cdot}NH_4PF_6$. The small $g$ anisotropy combined with the relatively small $^{14}N$ hyperfine splittings in $AgLNO_3^+$ indicate extensive delocalization involving the nitrate ion. The ESR parameters and electronic transition energies are used to evaluate the bonding parameters in these and other silver(II) complexes of N-heterocyclic ligands. The redox stabilities of silver and copper complexes of hindered N-heterocycles are compared.

## Introduction

It is well-known that the +2 oxidation state of silver is stabilized by N-heterocyclic ligands.[1] There have been several ESR studies on $Ag(py)_4^{2+}$,[2] $Ag(bpy)_2^{2+}$,[2c,3] and $Ag(phen)_2^{2+}$ [2a,c] (py = pyridine, bpy = 2,2′-bipyridine, phen = 1,10-phenanthroline). Most of these studies have been confined to undiluted polycrystalline samples and frozen aqueous solutions. With the exception of those of $Ag(py)_4^{2+}$ doped into $Cd(py)_4(ClO_4)_2$,[2a,b] silver and nitrogen hyperfine splittings are (partially) resolved only in frozen solutions. It has been recently pointed out that dissociation of one of the ligands occurs in solution, which complicates the analysis of such spectra.[2a] There has been no report on the isolation and characterization of silver(II) complexes of the sterically hindered ligands 6,6′-dimethyl-2,2′-bipyridine and 2,9-dimethyl-1,10-phenanthroline, abbreviated as dmbp and dmp, respectively. These

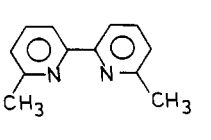

dmbp

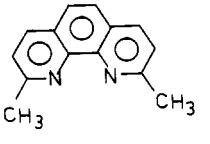

dmp

(1) (a) Levason, W.; Spicer, M. D. *Coord. Chem. Rev.* **1987**, *76*, 45. (b) Po, H. N. *Ibid.* **1976**, *20*, 171. (c) McMillan, J. A. *Chem. Rev.* **1962**, *62*, 65.
(2) (a) Evans, J. C.; Gillard, R. D.; Lancashire, R. J.; Morgan, P. H. *J. Chem. Soc., Dalton Trans* **1980**, 1277. (b) Buch, T. *J. Chem. Phys.* **1965**, *43*, 761. (c) McMillan, J. A.; Smaller, B. *Ibid.* **1961**, *35*, 1698. (d) Hecht, H. G.; Frazier, J. B., III. *J. Inorg. Nucl. Chem.* **1967**, *29*, 613.
(3) (a) Halpern, T.; McKoskey, S. M.; McMillan, J. A. *J. Chem. Phys.* **1970**, *52*, 3526. (b) Thorpe, W. G.; Kochi, J. K. *J. Inorg. Nucl. Chem.* **1971**, *33*, 3962.

0020-1669/89/1328-0662$01.50/0 

ligands are of special importance because of their ability to form stable copper(I) complexes having rich charge-transfer spectra.[4] It is therefore interesting to compare their complexing ability toward copper(I,II) and silver(I,II). We now report the isolation of the magnetically dilute salts $[AgLNO_3]PF_6 \cdot NH_4PF_6$, with L = dmbp and dmp, from oxidized solutions of the complexes of these ligands with silver nitrate. These two compounds gave well-resolved ESR spectra in the solid state, which were used to determine the bonding parameters in these novel silver(II) complexes.

## Experimental Section

dmbp was prepared by an earlier known procedure,[5] and dmp was purchased from Aldrich and recrystallized from methanol. All other chemicals were of reagent grade.

$Ag(dmbp)NO_3$[6] and $Ag(dmp)NO_3$[7] were obtained as white crystalline precipitates by mixing together, in 1:1 molar porportions, an aqueous solution of silver nitrate and a methanol solution of the ligand. The complexes were recrystallized from 0.1 N nitric acid, washed with water, and dried under vacuum. Anal. Calcd for $Ag(dmbp)NO_3$, $AgC_{12}H_{12}N_3O_3$: C, 40.7; H, 3.4; N, 11.9. Found: C, 40.5; H, 3.4; N, 11.6. Calcd for $Ag(dmp)NO_3$, $AgC_{14}H_{12}N_3O_3$: C, 43.3; H, 3.1; N, 10.9. Found: C, 43.6; H, 3.2; N, 11.0.

$[Ag(dmbp)NO_3]PF_6 \cdot NH_4PF_6$ and $[Ag(dmp)NO_3]PF_6 \cdot NH_4PF_6$ were prepared by similar procedures, described as follows for the former salt. Solid $Ag(dmbp)NO_3$ was added to an aqueous solution of $(NH_4)_2S_2O_8$ at −20 °C. The color slowly changed to brown, and the solid went into solution. A small amount of brown precipitate that formed was filtered off, and a cold aqueous solution of $NH_4PF_6$ was added. The light brown solid that precipitated immediately was separated by centrifugation, washed with ice-cold water, and dried under vacuum. Anal. Calcd for $AgC_{12}H_{16}F_{12}N_4O_3P_2$: C, 21.8; H, 2.4; N, 8.5; $Ag^{2+}$, 16.3; Ag, 16.3; dmbp, 27.8. Found: C, 22.6; H, 3.4; N, 9.0; $Ag^{2+}$, 16.8; Ag, 16.2; dmbp (spectrophotometry), 32. IR (in KBr disk) (prominent bands other than those due to dmbp): 3210 (s, b; $NH_4^+$), 1455 (s; $NO_3^-$), 1275 (m; $NO_3^-$), 820 $cm^{-1}$ (vs, b; $PF_6^-$) (vs = very strong, s = strong, m = medium intensity; b = broad). Electronic spectrum (PAS with $MgCO_3$ as diluent): $\nu_{max} = 18.9 \times 10^3$ $cm^{-1}$. The samples were hygroscopic. For ESR measurements, they were sealed under nitrogen in quartz tubes.

**Measurements.** IR spectra in the range 600–4000 $cm^{-1}$ were recorded on a Perkin-Elmer IR 1310 or IR 297 instrument. Electronic absorption spectra were recorded on a Perkin-Elmer LAMBDA-3 spectrometer or a PAR photoacoustic spectrometer. C, H, N analyses were performed by Bhaskar Rao on a Perkin-Elmer 240C analyzer. $Ag^{2+}$ was estimated by iodometric titration,[8] and total silver, by gravimetry.[8] Ligand percentage was determined by a spectrophotometric method using a Schimadzu UV–vis spectrophotometer ($\epsilon_{288nm} = 0.2483 \times 10^5$ $dm^3$ $mol^{-1}$ $cm^{-1}$ for dmbp in methanol). ESR spectra were recorded on a JEOL FE-3X spectrometer equipped with a variable-temperature cryostat.

***Computer Simulation of ESR Spectra.*** Polycrystalline spectra were simulated by using a previously described computer program[9] that was modified to include ligand hyperfine interaction in first order. The Hamiltonian employed was

$$\mathcal{H} = \beta_e \vec{H} \cdot \mathbf{g} \cdot \vec{S} + \vec{I} \cdot \mathbf{A} \cdot \vec{S} - g_n \beta_n \vec{H} \cdot \vec{I} + \vec{I}_{N1} \cdot \mathbf{A}_{N1} \cdot \vec{S} + \vec{I}_{N2} \cdot \vec{A}_{N2} \cdot \vec{S} \quad (1)$$

For the present compounds, **g** and **A** turned out to be axially symmetric. The nitrogen hyperfine tensors were assumed to be equivalent and axial, with the Ag–N bond direction as the symmetry axis. For planar coordinaton, this would mean that $A_\parallel$ for silver is in the $(x,y)$ planes of the nitrogen tensors. The resultant hyperfine constants $A$ and $B$ are related to $A_\parallel(N)$ and $A_\perp(N)$ as

$$A_\parallel(N) = B \qquad A_\perp(N) = (1/2^{1/2})(A^2 + B^2)^{1/2} \quad (2)$$

for square-planar configuration. The program has provision for any arbitrary orientation of the principal axis of the $^{14}N$ tensor, but the results are not sensitive to moderate distortions, due to the small hyperfine anisotropy. The calculations were performed on an IBM-compatible WIPRO Machines personal computer.

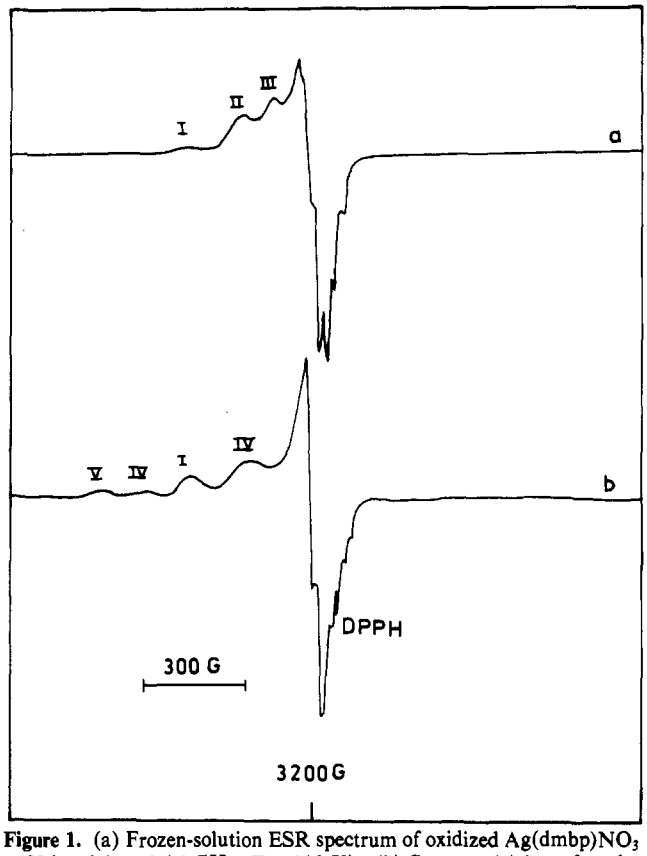


**Figure 1.** (a) Frozen-solution ESR spectrum of oxidized $Ag(dmbp)NO_3$ at X-band ($\nu$ = 9.26 GHz, $T$ = 113 K). (b) Same as (a) but after the glass was aged for 1 day.

## Results and Discussion

**Oxidation of $Ag(dmbp)NO_3$ and $Ag(dmp)NO_3$.** It is noteworthy that, unlike bpy and phen, dmbp and dmp form 1:1 complexes with $AgNO_3$. Persulfate oxidation of these compounds readily gives colored solutions. However, these solutions are rapidly decolorized on keeping at room temperature. This also is in contrast to the complexes of the unsubstituted ligands, which are smoothly oxidized to the stable solid compounds $[Ag(bpy)_2]S_2O_8$ and $[Ag(phen)_2]S_2O_8$.

The electronic spectra of the oxidized solutions have two maxima, one in the visible region and a much more intense one in the UV region, with the following transition energies ($10^3$ $cm^{-1}$): 18.9 and 31.6 for $Ag(dmbp)NO_3^+$; 23.5 and 31.0 for $Ag(dmp)NO_3^+$. The corresponding values for the complexes of the parent ligands are 22.0 and 34.1 for $Ag(bpy)_2^{2+}$[10] and 25.6 and 32.6 for $Ag(phen)_2^{2+}$.[2c] While the visible band arises from a d–d transition, the UV maximum is most likely dominated by a ligand to metal charge-transfer (LMCT) excitation. The reduced values of the transition energies could be either due to the lesser ligand field provided by dmbp (dmp) and $NO_3^-$ or due to the greater deviation of the coordination from planarity. This would mean that the highest occupied molecular orbital ($d_{xy}$) is at a lower energy in the nitrato complexes. This, as well as the red shift of the LMCT band, is consistent with their lesser stability. While $Ag(bpy)_2^{2+}$ is stable to reduction in aqueous solution ($E^\circ$ = 1.453 V),[11] the present complex ions are unstable even in strong nitric acid solution, implying a redox potential in the range 1.7–2.0 V.[12]

(4) (a) Day, P.; Sanders, N. *J. Chem. Soc. A* **1967**, *1530*, *1536*. (b) Burke, P. J.; McMillin, D. R.; Robinson, W. R. *Inorg. Chem.* **1980**, *19*, 1211. (c) Kitagawa, S.; Munakata, M.; Higashie, A. *Inorg. Chim. Acta* **1984**, *84*, 79.
(5) Newkome, G. R.; Pantaleo, D. C.; Puckett, W. E.; Ziefle, P. L.; Deutch, W. A. *J. Inorg. Nucl. Chem.* **1981**, *43*, 1529.
(6) Priscilla, K. M.Sc. Dissertation, University of Hyderabad, 1985.
(7) Hall, J. R.; Plowman, R. A.; Preston, H. S. *Aust. J. Chem.* **1965**, *18*, 1345.
(8) Bassett, J.; Denney, R. C.; Jeffery, G. H.; Mendham, J. *Vogel's Text Bok of Quantitative Inorganic Analysis*; ELBS: London, 1978.
(9) Rajasekharan, M. V.; Manoharan, P. T. *Mol. Phys.* **1981**, *44*, 1145.
(10) Banerjee, R. S.; Basu, S. *J. Inorg. Nucl. Chem.* **1964**, *26*, 821.
(11) Thompson, N. R. In *Comprehensive Inorganic Chemistry*; Trotman-Dickenson, A. F., Ed.; Pergamon Press: Oxford, England, 1973; Vol. 3, p 122.
(12) Greenwood, N. N.; Earnshaw, A. *Chemistry of the Elements*; Pergamon Press: Oxford, England, 1984; p 737.

**Table I.** ESR Parameters from Computer-Fit Spectra

| complex | $g_\parallel$ | $g_\perp$ | $10^4A_\parallel(^{107,109}Ag)$, $cm^{-1}$ | $10^4A_\perp(^{107,109}Ag)$, $cm^{-1}$ | $10^4A(^{14}N)$, $cm^{-1}$ | $10^4B(^{14}N)$, $cm^{-1}$ |
|---|---|---|---|---|---|---|
| $[Ag(dmbp)NO_3]PF_6 \cdot NH_4PF_6$ | 2.165 | 2.032 | 45.0 | 30.0 | 16.0 | 14.6 |
| $[Ag(dmp)NO_3]PF_6 \cdot NH_4PF_6$ | 2.194 | 2.037 | 47.5 | 24.0 | 25.0 | 15.8 |

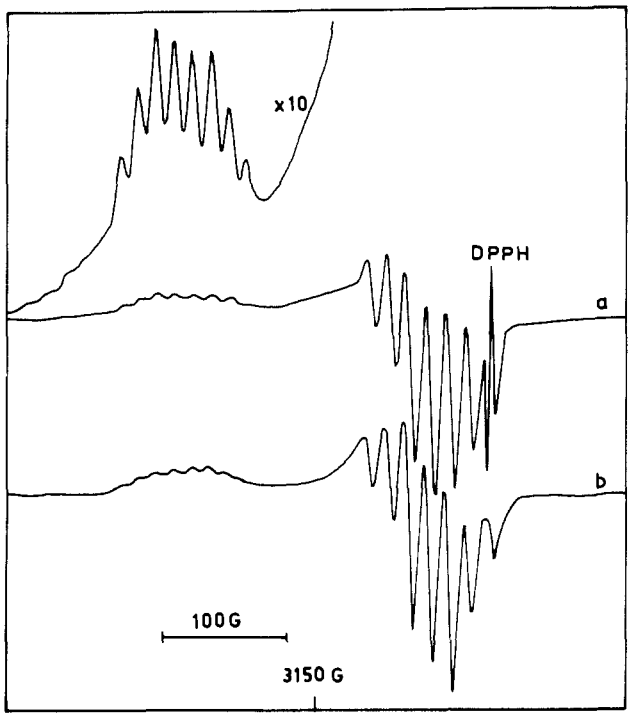


**Figure 2.** Polycrystalline ESR spectra of $[Ag(dmbp)NO_3]PF_6 \cdot NH_4PF_6$ at X-band ($\nu$ = 9.223 GHz, $T$ = 112 K): (a) experimental spectrum; (b) computer-simulated spectrum. The weak signals on the low-field side of the amplified portion are probably due to a weakly populated chemically inequivalent Ag(II) site.

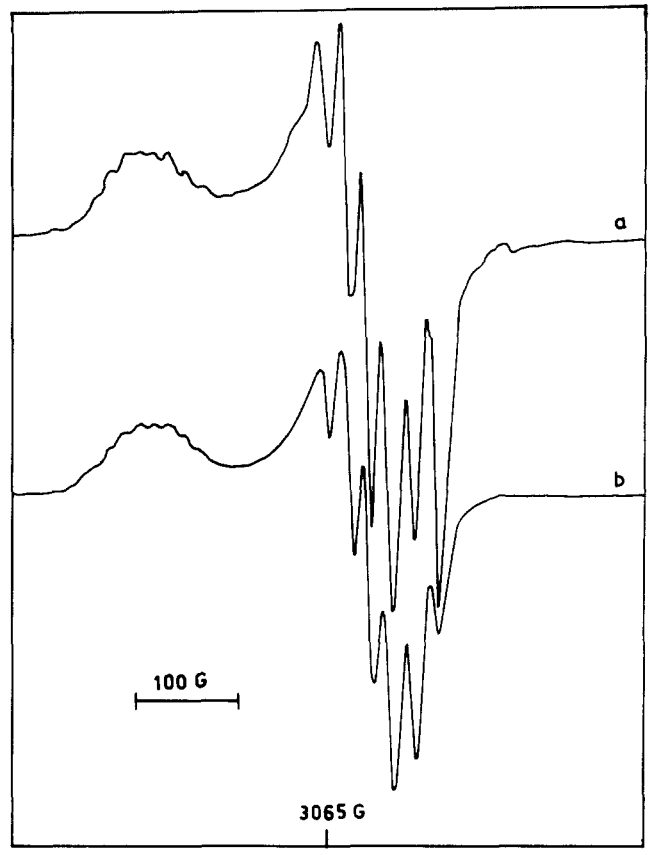


**Figure 3.** Polycrystalline ESR spectra of $[Ag(dmp)NO_3]PF_6 \cdot NH_4PF_6$ at X-band ($\nu$ = 9.220 GHz, $T$ = 153 K): (a) experimental spectrum; (b) computer-simulated spectrum. The signal from an unidentified organic radical, which was also present in the free ligand, dmp, is superimposed on the highest field line of the experimental spectrum.

The ESR spectra of frozen aqueous solutions resulting from the oxidation of $Ag(dmbp)NO_3$ are shown in Figure 1. At least three chemically inequivalent sites are clearly seen in the parallel region of the spectrum obtained with freshly prepared solutions. The weak signal I with $g_\parallel$ = 2.336 is assigned to the aqua ion of silver(II). The nuclear hyperfine splitting is not resolved in the parallel region due to the high concentration of the solutions used. Sites II ($g_\parallel$ = 2.217) and III ($g_\parallel$ = 2.153) should therefore correspond to different silver(II) complex ions containing the dmbp ligand, nitrate ion, and/or water molecules. When the frozen solution was aged for 1 day, species III completely disappears, the aqua ion (I) gains in intensity, and two weak signals are seen at $g_\parallel$ = 2.449 (IV) and $g_\parallel$ = 2.574 (V). The high $g$ values of the latter two sites, which imply larger orbital angular momentum induced by spin–orbit coupling, could result from greater distortion of the coordination toward a tetrahedron or from weak axial coordination by water or nitrate ion. The perpendicular part of the spectrum is complicated by the near coincidence of the $g_\perp$ values of the various species and also by the presence of both silver and nitrogen nuclear hyperfine interactions. From the hyperfine splitting pattern one can conclude that the complex species contain at the most one coordinated heterocyclic ligand, the other coordination sites being occupied by one or more water molecules or nitrate ions.

The spectra of the double salts show well-resolved hyperfine structure due to one $^{107,109}Ag$ ($I = {}^1/_2$) nucleus and two $^{14}N$ ($I$ = 1) nuclei (Figures 2 and 3). It is therefore clear that both in solution and in the solid state only one heterocyclic ligand is bound to silver. Further, the solid-state electronic spectrum (PAS) of $[Ag(dmbp)NO_3]PF_6 \cdot NH_4PF_6$ has an absorption band at the same energy ($18.9 \times 10^3$ $cm^{-1}$) as that observed in solution.

**Interpretation of the ESR Parameters of $Ag(dmbp)NO_3^+$ and $Ag(dmp)NO_3^+$.** The parameters derived from computer simulation are collected in Table I. Like all other silver(II) systems in magnetically dilute matrices, the present complexes also have an axial spin Hamiltonian. It has been demonstrated earlier in the case of bis(diethyldithiocarbamato)silver(II) that (near) axial symmetry does not necessarily imply degeneracy in the electronic energy levels.[13] While the symmetry of the $AgN_2O_2$ moiety cannot be higher than $C_{2v}(x)$, as is often the case, the electronic structure may be described in terms of $D_{2h}$ (planar) or $C_{2v}(z)$ (pseudotetrahedral) point groups. The higher values of the transition energies and greater delocalization of the odd electron are responsible for the reduced anisotropy in the case of the silver(II) complexes compared to similar complexes of copper(II). Among the silver(II) complexes of nitrogen heterocyclic ligands, those of dmp and dmbp have the smallest $g$ anisotropy. On the other hand, they have rather small $^{14}N$ hyperfine splittings. Therefore, the extensive $\sigma$- and $\pi$-delocalization implied by the small $g$ anisotropy is mainly taking place into the nitrate ion orbitals. This would suggest that $NO_3^-$ functions as a chelating ligand, which partly compensates for the weak interaction with the hindered heterocycles. The molecular orbital containing the odd electron (the HOMO) can be written as

$$\Psi_1 = \beta_1 d_{xy} - \beta_1' \Phi_{L1} \qquad (3)$$

where $\beta_1'\Phi_{L1} = c_1\Phi_{NN} + c_2\Phi_{NO_3^-}$ with $c_2^2 > c_1^2$. The other molecular orbitals, which are coupled to the HOMO via spin–orbit interaction, are $\Psi_2$ ($\beta_2 d_{x^2-y^2} - \beta_2'\Phi_{L2}$) and $\Psi_{3,4}$ ($\epsilon d_{xz,yz} - \epsilon'\Phi_{L3,4}$).

(13) Rajasekharan, M. V.; Sethulakshmi, C. N.; Manoharan, P. T.; Güdel, H. *Inorg. Chem.* **1976**, *15*, 2657.

**Table II.** Calculated Bonding Parameters[a]

| complex | $\Delta g_\parallel$ | $\Delta g_\perp$ | $10^{-3}E_{xy}$, cm$^{-1}$ | $10^{-3}E_{xz,yz}$, cm$^{-1}$ | $10^4A_F$, cm$^{-1}$ | $10^4A_D$, cm$^{-1}$ | $10^4A_\parallel^{(1)}$, cm$^{-1}$ | $10^4A_\perp^{(1)}$, cm$^{-1}$ | $\beta_1^2$ | $\beta_2^2$ | $\epsilon^2$ | $\kappa$ |
|---|---|---|---|---|---|---|---|---|---|---|---|---|
| $[Ag(dmbp)NO_3]PF_6 \cdot NH_4PF_6$ | 0.163 | 0.030 | 30.4 | 18.9 | 41.1 | 8.9 | −13.9 | −2.2 | 0.49 | 0.84 | 0.46 | 1.32 |
| $[Ag(dmp)NO_3]PF_6 \cdot NH_4PF_6$ | 0.192 | 0.035 | 31.1 | 23.5 | 38.6 | 12.3 | −15.6 | −2.2 | 0.68 | 0.71 | 0.42 | 0.896 |
| $[Ag(bpy)_2]S_2O_8$[b] | 0.208 | 0.045 | 28.0 | 22.0 | 39.0 | 10.1 | −17.3 | −2.9 | 0.56 | 0.84 | 0.62 | 1.10 |
| $Ag(phen)(NO_3)_2$[c] | 0.212 | 0.046 | 31.1 | 25.6 | 34.4 | 8.1 | −14.9 | −2.8 | 0.45 | 1.00 | 0.89 | 1.22 |
| $[Ag(py)_4]S_2O_8/[Cd(py)_4]S_2O_8$ | | | | | | | | | | | | |
| A[d] | 0.202 | 0.040 | 22.0 | 20.4 | −14.4 | 18.0 | −14.8 | −2.1 | >1[e] | 0.32 | 0.24 | −0.228 |
| B[f] | 0.178 | 0.038 | 22.0 | 20.4 | 33.0 | 8.5 | −16.0 | −2.6 | 0.47 | 0.74 | 0.62 | 1.12 |
| $Ag(TPP)/(H_2O)Zn(TPP)$[g] | 0.106 | 0.035 | 36.7 | 43.7 | 48.1 | 12.0 | −9.6 | −2.1 | 0.66 | 0.51 | 0.74 | 1.15 |

[a] Calculated with $\lambda = -1840$ cm$^{-1}$, $P = -63.0 \times 10^{-4}$ cm$^{-1}$, $S_1 = 0.1$, $S_2 = 0.0$, $S_{3,4} = 0.05$, and $T = 0.33$. $A_\parallel$ and $A_\perp$ were taken to be positive, except for the values for $Ag(py)_4S_2O_8/Cd(py)_4S_2O_8$ (A), for which the results quoted are for $A_\parallel > 0$, $A_\perp < 0$. [b] In frozen $HNO_3$; ref 3a (ESR) and 10 (optical spectra). [c] In frozen $HNO_3$; ref 2a (ESR) and 2c (optical spectra). [d] References 2a (ESR) and 1b (optical spectra). [e] Not physically meaningful. Other sign combinations for $A_\parallel$ and $A_\perp$ also fail to give meaningful results. [f] References 2b (ESR) and 1b (optical spectra). [g] References 17 (ESR, ENDOR) and 18 (theoretical estimates of transition energies).

If the Abragam–Pryce Hamiltonian and second-order perturbation theory are used, the **g** and silver **A** tensor components can be written as[14,15]

$$\Delta g_\parallel = g_\parallel - g_e = 8E_\parallel\beta_1^2\beta_2^2k_\parallel$$

$$\Delta g_\perp = g_\perp - g_e = 2E_\perp\beta_1^2\epsilon^2k_\perp$$

$$A_\parallel = A_F + 2A_D + A_\parallel^{(1)}$$

$$A_\perp = A_F - A_D + A_\perp^{(1)} \quad (4)$$

where $g_e = 2.0023$, $E_\parallel = \lambda/(E_1 - E_2)$, $E_\perp = \lambda/(E_1 - E_{3,4})$, $k_\parallel = 1 - (\beta_1'/\beta_1)S_1 - (\beta_1'\beta_2'/2\beta_1\beta_2)T$, $k_\perp = 1 - (\beta_1'/\beta_1)S_1 - (\beta_1'\epsilon'/2\beta_1\epsilon)T$, $A_F = -\beta_1^2P\kappa$, $A_D = (-2/7)\beta_1^2P$, $A_\parallel^{(1)} = -8E_\parallel\beta_1^2\beta_2^2 - (6/7)E_\perp\beta_1^2\epsilon^2$, and $A_\perp^{(1)} = (-22/14)E_\perp\beta_1^2\epsilon^2$. $S_1$ is the overlap integral for $\Psi_1$, and $T$ is related to the orbital angular momentum matrix elements for the ligand part of the molecular orbitals involved. $\lambda$ is the free-ion spin–orbit coupling constant and $P = g\beta g_n\beta_n\langle r^{-3}\rangle_{d_{xy}}$. The Fermi contact parameter, $\kappa$, is here defined as $\beta_1^2\kappa = (-8\pi/3)\{|\Phi_\uparrow(0)|^2 - |\Phi_\downarrow(0)|^2\}/\langle r^{-3}\rangle_{d_{xy}}$. The bonding parameters calculated by using eq 4 are included in Table II. It is seen that the odd electron is delocalized to the extent of 35–50%. There is also extensive $\pi$-interaction involving $d_{xz}$ and $d_{yz}$ orbitals.

The lower values of the d–d transition energies for the dmbp complex compared to the dmp complex imply a greater tetrahedral distortion. This distortion as well as a possible twisting of the bipyridyl ligand about the C–C single bond will considerably relieve the steric strain in $Ag(dmbp)NO_3^+$. A greater degree of metal–ligand interaction is therefore expected, and it is reflected in the lesser value of $\beta_1^2$ for this compound. The Fermi contact contribution to hyperfine splitting varies from 0.0033 to 0.0041 cm$^{-1}$ for the systems listed in Table II. The contact interaction is very sensitive to the 5s contribution, which in turn is usually a strong function of metal–ligand bond length.[16] In the absence of structural data and theoretical estimates, no attempt will be made here to explain the observed variation in $A_F$.

With reference to the nitrogen hyperfine splitting, the two components, $A$ and $B$, can be written as

$$A = f_{\sigma s}a_s + 2f_{\sigma p}a_p + 2A_D'$$

$$B = f_{\sigma s}a_s - f_{\sigma p}a_p - A_D' \quad (5)$$

where $a_s = (8\pi/3)g\beta g_n\beta_n|\Psi_0|^2$ and $a_p = (2/5)g\beta g_n\beta_n\langle r^{-3}\rangle_{2p}$, the atomic values being 0.051 79 and 0.001 55 cm$^{-1}$, respectively.[15] The correction due to direct dipolar interacton $A_D'$ is of the order of $1 \times 10^{-5}$ cm$^{-1}$ and can be neglected. The quantities $f_{\sigma s}$ and $f_{\sigma p}$ are the 2s and 2p electron densities for the HOMO. These data have often been used in the past to estimate the s:p hybridization ratio for the nitrogen $\sigma$ orital and even to calculate bond angles.[3a] However, the ratio depends on the difference $A$–$B$, which due to the proximity of $A$ and $B$ will often be subject to large errors. Further, the appreciable difference in the energies of the 2s and 2p orbitals and also any significant core polarization in the bonded nitrogen atom can further complicate the analysis. For $Ag(dmbp)NO_3^+$ and $Ag(dmp)NO_3^+$ we obtain 1.0 and 0.2, respectively, for the ratio $f_{\sigma s}/f_{\sigma p}$. The small s:p ratio for the dmp complex is evident in the unusually high anisotropy in the nitrogen hyperfine splitting. We postulate that the large p contribution relative to that of s is due to a much longer Ag–N bond, which favors greater interaction of the silver $\sigma$ orbitals with the nitrogen $2p\sigma$ orbital compared to the less diffuse 2s component.

A good system to compare with the simple N-heterocyclic ligands is porphyrin, which readily induces disproportionation of silver(I), forming silver(II) complexes with square-planar $N_4$ coordination. Single-crystal ENDOR studies on Ag(TPP) doped into $(H_2O)Zn(TPP)$, where $H_2TPP$ = tetraphenylporphyrin, have yielded very accurate metal and ligand hyperfine tensors for this system.[17] Subsequently, X$\alpha$ calculations have also been reported.[18] The data from our analysis of **g** and $^{109}$Ag hyperfine splitting are included in Table II. It has been pointed out that first-order perturbation treatment of **g** and metal hyperfine tensors gives less reliable bonding parameters than a zeroth-order analysis of the $^{14}$N hyperfine data, and the latter procedure is to be preferred whenever precise $^{14}$N coupling parameters are available.[17] We do find that the bonding coefficients are sensitive to transition energies. The low value of $\beta_2^2$ (0.51) implying greater in-plane $\pi$-bonding than $\sigma$- and out-of-plane $\pi$-bonding is unrealistic. $\beta_2^2$ is raised to 0.75 when $E_{xy}$ is raised by about 50%, while the other coefficients are not significantly modified. What is clear from the comparison of data in Table II is that the higher values of d–d transition energies in Ag(TPP) compared to those in other compounds are responsible for its lower $g$ anisotropy as well as the reduced magnitude of spin–orbit contribution to hyperfine splitting ($A_\parallel^{(1)}$ and $A_\perp^{(1)}$). Since the latter contributions are negative, the experimental hyperfine splitting values are considerably higher for Ag(TPP).

Finally, it may be mentioned that the recent analysis[2a] of the $Ag/Cd(py)_4S_2O_8$ is likely to be in error with regard to the silver hyperfine splitting because the assignment leads to unreasonable bonding parameters and a negative $A_F$ (Table II). We tend to favor the earlier analysis.[2b] The difference between the two lies in counting the numer of lines in the parallel region of the spectrum where 10 lines are expected if $A_\parallel(Ag) = A_\parallel(N)$ and 11 lines if $A_\parallel(Ag) = 2A_\parallel(N)$. However, we agree with Evans et al.[2a] that the nitrogen hyperfine splittings have to be revised. The revised values are also included in Table II.

**Comparison with Copper Complexes.** The bidentate N-heterocyclic ligands increase the $Cu^+/Cu^{2+}$ potential[19] from 0.167 to

(14) Manoharan, P. T.; Rogers, M. T. In *Electron Spin Resonance of Metal Complexes*; Yen, T. F., Ed.; Plenum Press: New York, 1968.
(15) Goodman, B. A.; Raynor, J. B. *Adv. Inorg. Chem. Radiochem.* **1970**, *13*, 135.
(16) Rajasekharan, M. V.; Bucher, R.; Deiss, E.; Zoller, L.; Salzer, A. K.; Moses, E.; Weber, J.; Ammeter, J. H. *J. Am. Chem. Soc.* **1983**, *105*, 7516.
(17) Brown, T. G.; Hoffman, B. M. *Mol. Phys.* **1980**, *39*, 1073.
(18) Sontum, S. F.; Case, D. A. *J. Phys. Chem.* **1982**, *86*, 1596.

0.251 V in the case of bpy and to ≳0.75 V for dmbp. The same ligands reduce the $Ag^+/Ag^{2+}$ potential from 1.9 to 1.45 V $(bpy)^{II}$ and to ≳1.7 V (dmbp, dmp). The major reason for the increase of the $Cu^+/Cu^{2+}$ potential is the tetrahedral distortion of the $CuL_2^{2+}$ ions, especially for the hindered ligands.[4] The unhindered ligands tend to form octahedral *cis*-$CuL_2(H_2O)_2^{2+}$ species in aqueous solution, which lowers the potential. On the other hand, the reduction in the $Ag^+/Ag^{2+}$ potential appears to be due to the extensive delocalization of charge via $\sigma$- and $\pi$-bonding interactions. Here again, the tetrahedral distortions in the case of dmbp and dmp complexes tend to raise the potential.

**Acknowledgment.** Financial support from the University Grants Commission to G.S. and from the Council of Scientific and Industrial Research, New Delhi, is acknowledged.

(19) James, B. R.; Williams, R. J. P. *J. Chem. Soc.* **1961**, 2007.

Contribution from the Department of Chemical Technology, Kanagawa Institute of Technology, 1030 Shimo-ogino, Atsugi, Kanagawa 243-02, Japan, and National Chemical Laboratory for Industry, Tsukuba, Ibaraki 305, Japan

# Microwave Spectra and Molecular Structures of 3*H*-3-Azacyclotriboroxane and 3-Oxacyclotriborazane

Yoshiyuki Kawashima,*[1a] Harutoshi Takeo,[1b] and Chi Matsumura[1b]

*Received September 29, 1988*

The species 3*H*-3-azacyclotriboroxane ($B_3H_4NO_2$) and 3-oxacyclotriborazane ($B_3H_5N_2O$) have been identified by microwave spectroscopy to be among the products of the reaction of diborane with nitrogen monoxide. The rotational constants obtained for the normal species are $A$ = 5663.80 (15), $B$ = 5616.39 (11), and $C$ = 2820.405 (15) MHz for $B_3H_4NO_2$, and $A$ = 5472.32 (10), $B$ = 5427.24 (9), and $C$ = 2725.013 (8) MHz for $B_3H_5N_2O$, with 3 standard deviations in parentheses. Analysis of the spectra for the normal, deuterated, $^{15}N$, and $^{10}B$ species leads to the structural parameters of the skeletal rings. The reaction mechanism for the formation of these molecules is discussed.

## Introduction

In the past several years many stable and unstable borane derivatives have been investigated by microwave spectroscopy in our laboratory, and the existence of new molecules has been established spectroscopically.[2-6] As an extension of the above study, we tried to detect a borane containing the NO group or NO groups by the reaction of diborane ($B_2H_6$) with nitrogen monoxide (NO).

The existence of $BH_3NO$ has been suggested by Hoffmann and Engelhardt on the basis of mass spectrometry.[7] They examined mixtures of $BH_3CO$ and NO by the use of mass spectrometry and demonstrated the possibility that $BH_3NO$ might exist as an intermediate during the formation of $N_2O$ and boric acid from $BH_3CO$ and NO. In the previous studies of the reaction products of diborane with water,[2] ammonia,[5] etc. by microwave spectroscopy, the borane derivatives tended to be detected rather than the addition complexes of borane. Therefore, we expected to detect $BH_2NO$ by the reaction of $B_2H_6$ with NO. However, a strong spectrum of $BH_2NH_2$ was observed and no spectrum due to $BH_2NO$ was found. It was not easy to understand the reaction mechanism of how the $BH_2NH_2$ was produced by the reaction of $B_2H_6$ with NO. Therefore, we investigated the products of this reaction carefully, and found new spectra in addition to those due to $BH_2NH_2$,[5] $B_2H_5NH_2$,[8] and $N_2O$.[9] Although the origins of the new spectra were difficult to deduce by consideration of the only possible reactions, they were identified to be 3*H*-3-aza-cyclotriboroxane ($B_3H_4NO_2$) and 3-oxacyclotriborane ($B_3H_5N_2O$) from the rotational constants and other information for the various isotopic species obtained by microwave spectroscopy. Similar molecules, boroxin[10] and borazine[11], are well-known, whereas there is no report of $B_3H_4NO_2$ and $B_3H_5N_2O$. The results of this study are reported herein.

## Experimental Section

A high-temperature reaction system using a flow-through method was adopted for the production and detection of the new molecules.[2] A mixture of $B_2H_6$ and NO was passed through a quartz tube heated by a nichrome wire coil and pumped continuously through a 3-m X-band brass wave-guide cell of a conventional 100-kHz Stark modulated spectrometer at a typical pressure of 20 mTorr. The quartz tube had an inner diameter of 4 mm, a thickness of 1.5 mm, and a length of 300 mm.

Optimum conditions for the production of new molecules were obtained when the temperature of the quartz tube was 450 °C and the mixing ratio of $B_2H_6$ and NO was about 1:2. This temperature was also optimal for the production of $BH_2NH_2$ and $B_2H_5NH_2$, while a higher temperature was advantageous for the production of $N_2O$. The spectra of the $^{10}B$ species were observed in their natural abundances. The spectra of the D and $^{15}N$ species were obtained by using $B_2D_6$ and $^{15}NO$, respectively. All measurements were carried out with the cell cooled to about −20 °C. The spectral intensity of $B_3H_5N_2O$ was always weaker than that of $B_3H_4NO_2$; the intensity ratio was about 1:2.

When the reaction products were closed in the cell by stopping the flow-through system, the spectra of both molecules decreased gradually and disappeared in several minutes. However, it is not certain that they are essentially unstable transient molecules because the deposition of the reaction products might affect the stability of the molecules.

## Results

**Analysis of the Spectra.** Survey scans of the 30–50-GHz region showed spectra due to $BH_2NH_2$, $B_2H_5NH_2$, and $N_2O$. In addition, condensed bunches of spectra consisting of a characteristic Q-branch series from a nearly symmetric rotor were observed at 31.0, 36.7, 42.3, and 48.0 GHz. An example of an observed Q-branch series is shown in Figure 1. The Q-branch series lines showed a slight intensity alternation due to spin weights, suggesting the existence of $C_2$ symmetry. No a-type R-branch series with a characteristic nearly prolate symmetric top pattern was observed in spite of a careful search. These facts suggest that the molecule in question is a planar oblate nearly symmetric top. Therefore, R-branch transitions were searched for and found by using the values of $A-C$ and $\kappa$ derived from the analysis of the Q-branch transitions and the assumption that $A \approx B \approx 2C$.

* To whom correspondence should be addressed.

(1) (a) Kanagawa Institute of Technology. (b) National Chemical Laboratory for Industry.
(2) Kawashima, Y.; Takeo, H.; Matsumura, C. *J. Chem. Phys.* **1981**, *74*, 5430.
(3) Kawashima, Y.; Takeo, H.; Matsumura, C. *Chem. Phys. Lett.* **1978**, *57*, 145.
(4) Kawashima, Y.; Takeo, H.; Matsumura, C. *J. Mol. Spectrosc.* **1979**, *78*, 493.
(5) Sugie, M.; Takeo, H.; Matsumura, C. *Chem. Phys. Lett.* **1979**, *64*, 573.
(6) Kawashima, Y.; Takeo, H.; Matsumura, C. *J. Mol. Spectrosc.* **1986**, *116*, 23.
(7) Hoffmann, K. F.; Engelhardt, U. *Z. Naturforsch.* **1970**, *25B*, 317.
(8) Lau, K.-K.; Birig, A. B.; Beaudet, R. A. *Inorg. Chem.* **1974**, *13*, 2787.
(9) Coles, D. K.; Elysh, E. S.; Gorman, J. G. *Phys. Rev.* **1947**, *72*, 973L.
(10) Chang, C. H.; Porter, R. F.; Bauer, S. H. *Inorg. Chem.* **1969**, *8*, 1689.
(11) Harshgarger, W.; Lee, G. H.; Porter, R. F.; Bauer, S. H. *Inorg. Chem.* **1969**, *8*, 1683.

0020-1669/89/1328-0666$01.50/0 